INTERNATIONAL ATOMIC ENERGY AGENCY
UNITED NATIONS EDUCATIONAL, SCIENTIFIC AND CULTURAL ORGANIZATION

INTERNATIONAL CENTRE FOR THEORETICAL PHYSICS
34100 TRIESTE (ITALY) · P.O.B. 586 · MIRAMARE · STRADA COSTIERA 11 · TELEPHONE: 2240-1
CABLE: CENTRATOM · TELEX 460392-I

SMR/208 - 42

SPRING COLLEGE IN MATERIALS SCIENCE

ON

"METALLIC MATERIALS"

(11 May - 19 June 1987)

AMORPHOUS METALS

N.E. CUSACK
School of Mathematics and Physics
University of East Anglia
Norwich NR4 7TJ
U.K.

SPRING SCHOOL

OF THE

INTERNATIONAL CENTRE FOR THEORETICAL PHYSICS

Trieste, 11th May - 19th June 1987

Notes accompanying the lectures on Metallic Glasses

These "notes" are corrected proofs of Chapter 12 - "Metallic Glasses" - of a book to be published in September 1987: "The Physics of Structurally Disordered Matter : An Introduction" by N.E. Cusack. The proofs are available to the Spring School by courtesy of the publisher Adam Hilger, Ltd., Bristol, BS1 6NX, England.

12

THE STRUCTURE AND ELECTRONIC PROPERTIES OF METALLIC GLASSES

Metal physics acquired a new and rapidly growing branch when it became easy in the 1970s to fabricate metallic glasses and when technical applications were found for them. Since alloy glasses can be made with all kinds of metals, amorphous systems with many kinds of properties can be studied, for example, a wide variety of magnetic behaviour is obtainable.

So many metallic glasses have been studied that various attempts to classify them have been made. No particular classification scheme will be emphasised in the sections below, but for some purposes a systematisation can be valuable. In a major review, a division by magnetic properties was used by Mizutani (1983), whose five classes were: ferromagnetic, weakly ferromagnetic, spin glass and Kondo-effect types, paramagnetic, weakly paramagnetic and diamagnetic. The magnetic and all the other properties must depend on the nature of the constituents, and grouping by chemical composition is also very common. Let us designate classes of pure metals by letters: S, simple metal (in the sense of Chapter 6); T, transition metal; M, metalloid†; *R*, rare earth; N, noble metal. Then some binary glass groupings, with examples, would be: S-S (Ca-Mg, Zn-Al); T-M (Ni-B, Fe-P); N-T (Cu-Ti, Au-Co); T-T (Fe-W, Pd-Zr); R-T (Ni-Dy, Fe-Hf). Different values of x in A_xB_{1-x} will lead to different properties, indeed ferromagnetism or even metallic conductivity may be present for some concentrations and not others. Consequently, property and composition classifications cut across each other and at certain concentrations a T-M glass might have properties characteristic of the S-S group. Many glasses, including some of practical utility, will be ternary, or more complicated still.

As with amorphous semiconductors, the realisation of technical applications has stimulated research into glassy alloys. Mechanical and anticorrosion properties are valuable but it would probably be true to say that up to the mid-eighties most commercial applications have exploited the magnetism in such devices or processes such as in recording, recorder heads, transformer cores, permanent magnets, shielding, transducers and sensors. This chapter will not deal with the technical applications; many pertinent papers can be found in Steeb and Warlimont (1985).

†In chemistry a metalloid is an element with properties intermediate between those of metals and non-metals. The class is not perfectly well defined but usually includes B, P, Ge, Si, As, Sb, Te.

12.1 Formation of metallic glasses

It is not easy to make amorphous metallic elements. By receiving evaporated Bi or Ga atoms on a cooled substrate, non-crystalline solid films were made by Bückel in the fifties, and Wright and colleagues did this with Co in 1972. Liquid quenching of glassy Ni was reported by Davies *et al* in 1973. But it is much easier to make liquid alloys into glasses, and a major step was taken with the discovery of splat cooling by Duwez and collaborators in 1959. This technique uses the impact of liquid droplets on a cooled highly conducting target to produce rapid quenching, say 10^6 K s^{-1}, resulting in a small foil of metallic glass. It soon became clear that many alloys could be vitrified in this way and, as interest grew in their properties, other quenching techniques evolved.

Several families of methods exist for making non-crystalline solid alloys. One is deposition 'atom by atom' from gaseous or liquid phases as in sputtering, evaporation or electrodeposition. Another is ion implantation or particle bombardment. Mechanical cold working of foils or powders can also be effective and a fourth approach is to cause amorphisation reactions to occur in the solid state; it even appears possible to convert $Cr_{1-x}Ti_x$ from amorphous to crystalline and back by thermal cycling (Blatter and von Allman 1985). However, the most widely exploited method is quenching from the melt and this family includes splat cooling, melt spinning and laser glazing (Beck and Güntherodt 1983, Luborsky 1983).

Laboratory equipment suitable for melt spinning research samples is shown in figure 12.1. An air or helium stream impinging on the buckets drives the roller to a rim surface speed of, say, 30 m s^{-1} normally at room temperature. Then the He injection pressure operates to squirt the alloy—now made molten by the induction winding—against the copper rim of the roller where a ribbon of amorphous alloy forms (Pavuna 1981). In other versions the molten metal is aimed at the narrow gap between two cold oppositely rotating rollers or at a chilled metal belt at the point where the belt itself passes between oppositely moving rollers. Since amorphous metal ribbons have become a significant commercial product, devices for continuous fabrication are being developed all the time. (See, e.g. many papers in Steeb and Warlimont 1985, Suzuki 1982).

As with amorphous semiconductors there is the question of whether the characteristics of a sample depend on its mode of preparation and, as the result is a solid out of thermodynamic equilibrium, the answer must in general be yes. The properties may then alter after fabrication; indeed many properties can be observed to change with time in samples held at a constant annealing temperature. For example, over some hundreds of hours, lengths may contract slightly, Young's modulus determined by sound velocity may increase a few per cent, viscosity measured by creep may rise, internal stresses fall, and so on. Electrical and magnetic properties change also. The

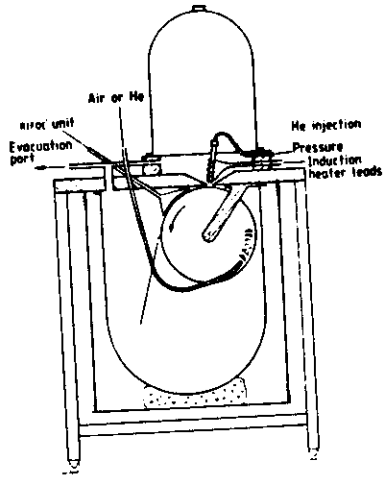

Figure 12.1 Schematic diagram of melt-spinning apparatus (from Pavuna 1981). RIFOC—ribbon fly-off control unit for secondary cooling and ribbon trajectory.

final value attained by a property depends on the annealing temperature. Presumably adjustments, some of an irreversible kind, proceed in the nearest-neighbour distances, altering both topological and chemical arrangement and acting to reduce overall disorder. Looked at from a free-volume point of view (§10.4), the free volume changes in amount and distribution. With very accurate diffraction studies made to large Q, such changes may be detectable in the radial distribution functions (Sifrolovitz *et al* 1981). Changes of properties with time must always be a consideration in technical applications and, if not allowed for, might vitiate comparisons of measurements made of samples of different age.

When a liquid alloy is quenched, vitrification competes with crystallisation and possible crystalline outcomes are homogeneous solid solutions or mixtures of two or more solutions or intermetallic compounds. As more and more alloys were vitrified it became clear that some alloys form glasses more readily than others and that some composition ranges are particularly favourable. Ready glass formation, or good glass-forming ability (GFA), means that the minimum rate of cooling, R_c, required to form a glass is relatively low, say less than about 10^5 K s^{-1}.

It was observed that the range of ready glass formation often embraced

deep eutectic points (figure 12.2(*a*)). The low value of the liquidus temperature, T_L, at a eutectic point indicates a comparatively high stability of the liquid phase relative to the solid at that composition. The glass transition temperature, T_G, may be regarded as a measure of the stability of the glass: the higher T_G, the more stable the glass is. T_G is relatively insensitive to composition in a binary alloy but T_L frequently depends strongly on concentration. The reduced glass transition temperature, $T_{RG} \equiv T_G/T_L$, is often used as an index of glass-forming ability and has high values, say greater than about 0.6, at compositions where stable glasses (high T_G) can form near

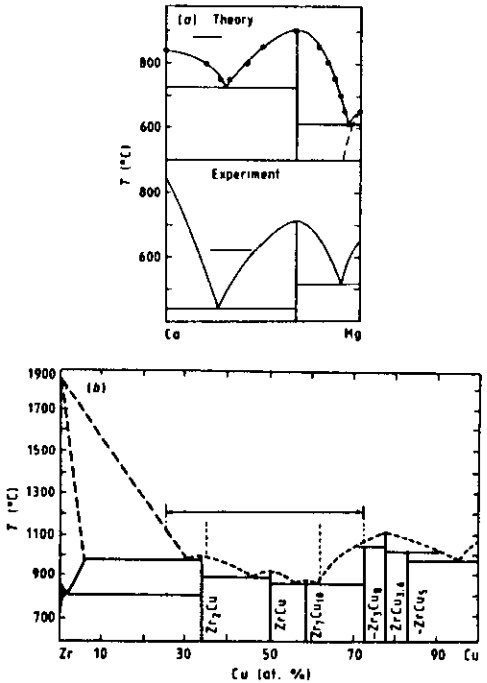

Figure 12.2 Equilibrium phase diagrams of (*a*) Ca–Mg. (After Hafner (1983) ~~combined with information from Giessen (1982)~~.) (*b*) Cu–Zr, with eutectic points. Glass-forming ranges are shown by the horizontal lines above the liquidus. (From Giessen and Wang 198X.)

deep eutectic points or, more generally, where T_L is low (figure 12.2(*b*)). T_G is not always known or easy to measure; sometimes the crystallisation temperature of the glass, T_{CR}, is used as an alternative index of glass stability.

An interesting and pertinent question to raise is: for a given material at a specified temperature how long does it take for a melt to nucleate and grow crystals to the extent that a very a small volume fraction, say 10^{-6}, is crystalline? This time would be expected to be very long at high temperatures where the liquid is stable and very long at low temperatures where the atomic mobility controlling nucleation and growth from the supercooled melt is very low. At some intermediate temperature the degree of supercooling will be optimum for crystallisation. These qualitative ideas can be expressed by time–temperature-transformation (TTT) curves such as the schematic one shown in figure 12.3(*a*) and the others shown in 12.3(*b*) (Davies 1976). Calculating TTT curves is an exercise in homogeneous nucleation theory which we shall omit here; it involves hypotheses about both the probability of spontaneous formation of a nucleus and the rate of its growth. Diffusion coefficients, interfacial energy and free-energy differences between melt and crystal, as well as $T_L - T$, are all part of the input to the calculation and it is difficult to avoid numerous approximations. Once TTT curves are established however, it becomes possible to understand that R_c is a rate of cooling giving a vitrification trajectory which just grazes the vertex of the TTT curve (figure 12.3(*a*)). If, notionally, T_G is fixed and T_L varied, then the R_C's could be calculated form a series of TTT curves corresponding to different values of T_{RG} because different T_L would require different inputs to the TTT calculation. As might be expected, R_c falls through several orders of magnitude as T_{RG} varies from about 0.2 to about 0.7 (Davies 1976).

Apart from the presence of eutectics, a number of semiempirical criteria emerged for anticipating ready glass formation and some of these will be described. They are not necessary, still less sufficient, conditions for ready glass formation but they are possible contributory factors that seem to favour vitrification in some cases (see, e.g., Sommer in Steeb and Warlimont 1985).

When a range of composition embraces several relatively complex crystal structures, the liquidus may stay low and the glass-forming range be prolonged (figure 12.2(*b*)).

In an alloy A_xB_{1-x} a size difference may be very significant. Many glasses form with A = a noble or transition metal, B = a metalloid, and $x \simeq 0.75$ to $\simeq 0.85$. Much studied glasses like $Pd_{80}Si_{20}$, $Fe_{80}B_{20}$, $Ni_{20}P_{80}$ are examples. It was suggested that the dense random packing of the larger (A) component left interstices into which the smaller (B) atoms fitted—an idea compatible with $x \sim 0.8$. This may occur in some easily formed glasses but there are many counterexamples. Instead of, or as well as, size differences some chemical attraction between A and B may well help both to form and to stabilise glasses. When this is so, chemical short-range order (CSRO—see §§1.7, 2.7)

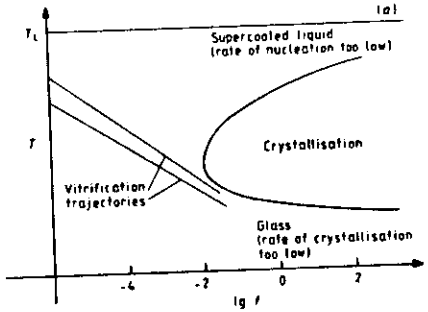

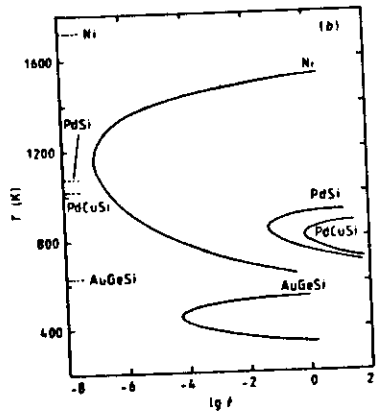

Figure 12.3 The TTT curves: (*a*), schematic; (*b*), derived for the systems shown for a 10^{-6} volume fraction of crystallisation (from Davies 1976). Broken lines show the liquidus temperature for various compounds.

should be detectable and this is often the case; examples are discussed in the next section.

The conduction electrons play such an important role in metals that an electronic criterion for glass formation might be looked for. It was offered by Nagel and Tauc (1975) who argued as follows on the basis of NFE theory. If Q_p is the position of the first peak of $S(Q)$, then $2k_F \simeq Q_p$ is a strong-scattering condition corresponding as nearly as may be to Bragg scattering in an

ordered structure. The energy $E_F \simeq \hbar^2(Q_p/2)^2(2m)^{-1}$ can therefore be assumed to be in a pseudogap with low $g(E_F)$ corresponding to the energy gap in a crystal (§9.10). However, $2k_F$ is determined by the valence electron density which is a function of composition and the requirement $2k_F = Q_p$ gives compositions for metal–metalloid systems about equal to those found for ready glass formation (e.g., $Pd_{80}Si_{20}$). The idea is that when E_F is in a pseudogap, and when structural fluctuations representing incipient crystallisation detract from the spherical symmetry in the liquid, the energy-lowering condition $2k_F = Q_p$ will cease to hold for all directions and an increase in energy will result. The liquid is thus metastable with respect to crystallisation and glasses tend to form easily as temperature falls. This explanation appears to work in some cases and the validity of considering the electronic energy cannot be doubted. But the dubiousness of using NFE concepts for systems with transition metals has been touched on before (§6.16) and evidence will be given below that E_F does not necessarily lie in a pseudogap.

It would be reasonable to assume that electron density, size differences and chemical affinity are all influences on glass formation. So is it possible to start from first principles and understand why certain ranges of composition are conducive to easy glass formation? Expressed thermodynamically, why are the free energies of the crystalline alternatives not so much lower than that of the supercooled liquid that crsytallisation inevitably occurs? The theory of metals given in Chapter 6 ought to be able to answer this at least for simple metals and that it could do so was first demonstrated by Hafner (1980) for Ca–Mg. It is an aspect of the general problem of calculating alloy phase diagrams from first principles and this requires an evaluation of ΔG, ΔH or ΔF as functions of composition (see §6.9 for the definitions of quantities like ΔG). Once $\Delta G(c)$ is found for various temperatures, there is a routine procedure in metallurgy for deducing the phase diagram from the principle that phases in equilibrium have equal chemical potentials (Hume-Rothery *et al* 1952).

Suppose that screened pseudopotentials have been constructed for the two metals at a given alloy composition and the corresponding electron density. As shown in §6.7 effective pair potentials follow from this. A number of techniques are then available for computing the structure and thermodynamic functions of the liquid alloy and these have been introduced before, namely, MD and MC (§§4.1, 4.2), GB, WCA and other variations and perturbation methods (§§5.8, 6.9). Such computations, based for example on a hard-sphere reference system, can lead *inter alia* to $\Delta G(c, T)$, $\Delta S(c, T)$ and $S_i(Q)$ (§6.9). In the particular case of liquid Ca–Mg the results are in very reasonable agreement with experiment. There are, in addition, two approaches to the structure of the glassy state: the liquid computations could be repeated for $T \ll T_L$; or a cluster relaxation calculation could be done starting with a DRP cluster and relaxing it using the pair potentials (see §§2.5, 8.5). These two approaches lead to very similar, but not identical, results for

$g_{ij}(r)$, the difference showing up particularly in the second peak which is split in the cluster derivation (as often in experiments) but not in the other. A reasonable approximation to $\Delta G(c, T)$ etc. can therefore be derived for the glass by treating it as a supercooled liquid. It remains to consider the crystalline phases.

As the phase diagram of Ca–Mg shows (figure 12.2(*a*)), the compound relevant to glass formation is $CaMg_2$. With carefully constructed pseudopotentials it is possible to calculate the total energy (both volume and structure terms; equation (6.31)) for any assumed crystal structure and lattice parameters, and to vary both to identify the ground state. For the energetically preferred structure and lattice constants, the values of ΔU and ΔV could be found. At finite temperatures the contribution of lattice vibrations to the thermodynamic properties must be added in and can be estimated from a Debye model. In principle, many conceivable crystal structures at different compositions could be investigated this way to discover what intermetallic compounds would exist but, in Ca–Mg, other possibilities, such as Ca_2Mg, turn out to be relatively unstable and irrelevant to the present considerations. For a range of compositions in which some Ca is in equilibrium with some $CaMg_2$, the free energy is the sum of the two contributions. Conceivably, however, a solid solution might have formed instead, and $\Delta G(c)$ for this can also be computed from the pseudopotentials: in practice in the Ca–Mg system, the hypothetical solid solution turns out to have a high positive energy of formation and therefore to be energetically unfavourable compared with a mixture of Ca and $CaMg_2$.

What has just been described is the structure in outline of a very extensive calculation of which details are given by Hafner (1980). One outcome is the calculated phase diagram in figure 12.2(*a*) which is in qualitative agreement with the measured one. But because ΔG of supercooled liquids is also calculated, the range (if any) of composition where ΔG (supercooled liquid) is close to ΔG (Ca + $CaMg_2$ mixture) can be identified. We expect this to be the range in which—if rates of cooling are favourable—the supercooled liquid is likely to vitrify before crystallisation occurs. This range is shown in figure 12.4 where the ready-glass-forming range reveals itself near the eutetic. This establishes that, subject to the numerous approximations of a first-principles calculation, a rational basis exists for understanding why ready-glass-forming regions exist where they do. The electronic ingredients of pseudopotential theory, which lead to interionic potentials like those of §§4.5 and 6.7, automatically imply size differences (positions of ion–ion potential minima), chemical interactions (screening charges, charge transfer) and valence electron densities which all collectively determine the run of $\Delta G(c)$ curves and so ultimately the glass-forming ability. No doubt it will be difficult to demonstrate this in detail for more complicated glasses especially those with transition metal constituents; Ca–Mg is a relatively simple case used here to illustrate the possibilities of first-principles explanations.

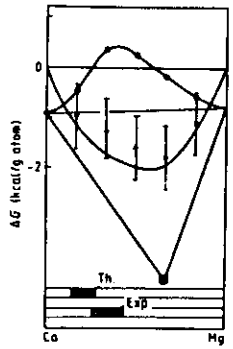

Figure 12.4 ΔG (in kcal per gm atom) calculated for Ca–Mg at 420 °C. Crosses with error bars show the theoretical ΔG of the supercooled liquid or glass and the curve through them is a possible interpolation. Full curves refer to a hypothetical solid solution. Sloping straight lines are linear interpolations of ΔG between the end points, the lowest end point being $CaMg_2$. The hatched regions indicate glass formation. (From Hafner 1980.)

12.2 Structure and vibrational spectrum

In the structural spread between dense random packing of hard-spheres ~~networks~~ (DRPHS) and covalent networks with low coordination (CRN), metallic glasses lie towards the former. The investigation of their LRO and SRO by diffraction, EXAFS and other techniques, and its representation by modelling and computation, are not essentially different from what has been described in earlier chapters either in general terms (Chapters 2, 3, 4 and 8) or in relation to insulating or semiconducting glasses (Chapters 10 and 11). Indeed metallic glasses have been taken as examples in §§2.5, 2.6, 2.7, 3.11, 3.13 and 8.5. This section therefore simply supplements what has gone before by a small number of additional examples. The primary problems are to obtain partial pair distribution functions, or equivalent information, and some insight into SRO. Good quality diffraction experiments, though difficult, will yield S_{NN}, S_{Nc}, S_{cc} or the S_{ij}. Ingenious use of null elements or zero alloys (§3.11), the combination of neutron work with x-ray work, and judicious choices of composition and concentration, can all lead to separate partial structure factors.

In an extensive study of melt-spun CuTi glasses, Sakata *et al* (see Suzuki (1982) p 330) demonstrated interesting relations between chemical short-range order (CSRO) and certain measures of stability in the glass and also

established that CSRO in the liquid exists before vitrification. In this particular system, S_{Ni} is negligible and the difference between the values of the $|f(Q)|^2$ for x-rays and the $|b|^2$ for neutrons is large enough to give two simultaneous intensity equations soluble for S_{cc} and S_{NN} (see equation (3.32)). Coordination numbers, nearest-neighbour distances and SRO parameters, η, all follow from this for each of seven compositions. $\eta = \eta_{AB} = \eta_{BA}$ as defined in §2.7, and a positive value shows that CSRO exists and unlike neighbours are preferred. Figure 12.5 shows η as a function of composition and also its strong positive correlation with T_{CR} and T_{CR}/T_L. Here, T_{CR} is being used instead of T_G as a measure of glass stability and T_{CR}/T_L is thus a measure of glass-forming ability. It appears clearly that stability, glass-forming ability and CSRO go together. It would be somewhat surprising if the CSRO were completely absent in the liquid state and the experiment showed that it is there but that vitrification enhances η by a factor of at least two (Sakata *et al* 1981, Cowlam *et al* 1984).

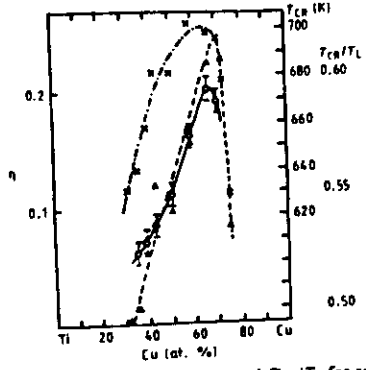

Figure 12.5 Chemical SRO parameter (η), T_{CR} and T_{CR}/T_L for some Cu–Ti glasses. ●, η; —·—·—, T_{CR}; -▲--, ▲ T_{CR}/T_L. (From Cowlam *et al* in Suzuki 1982.)

Melt-spun metal–metalloid glasses are among the most widely studied amorphous metals and when they involve Ni it is possible to use ^{0}Ni which stands for the null isotopic mixture with zero coherent neutron scattering length. Isotopic substitution is possible for Fe, and neutron scattering can be supplemented by x-rays. Combining these possibilities, Lamparter *et al* derived partial structure factors for $Ni_{81}B_{19}$, $Fe_{80}B_{20}$, $Co_{81.5}B_{18.5}$ and inferred the $g_{ij}(r)$'s. Of the various results, figure 12.6 shows the $S_{ij}(Q)$ of the Fe-B

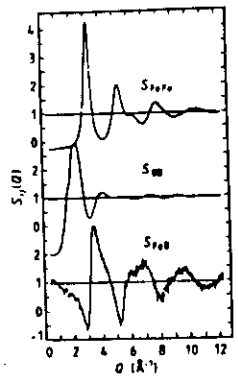

Figure 12.6 Partial structure factors of amorphous $Fe_{80}B_{20}$. (From Lamparter *et al* in Suzuki 1982.)

system. The resulting curve for $g_{FeB}(r)$ showed a strong narrow first peak implying a well defined Fe–B distance and therefore presumably a chemical bond. In the Ni–B system, $S_{B\text{-}B}(Q)$ is obtainable directly if ^{0}Ni is used and the corresponding g_{BB} had a split first peak indicating two separate B–B distances (Lamparter *et al*, in Suzuki (1982), p 343). Partial coordination numbers (see §2.4) are given in table 12.1 and the SRO parameter, η_{AB} (see §2.7), for $Fe_{80}B_{20}$ is unity indicating complete chemical ordering. Studies of $Ni_{80}P_{20}$ give comparable but not identical results (see Steeb and Warlimont (1985) p 459).

Table 12.1 Partial coordination numbers in T–B systems.

	T	B
T = Fe	12.4	2.2
B	8.6	6.5
T = Co	12.7	1.5
B	6.6	—
T = Ni	10.8	2.2
B	9.3	3.6:3.7†

†Under the two separate peaks.

As a final example we take an R-T glass, namely, Dy_7Ni_3. It happens that both elements can be isotopically mixed to null form and first 'double-null' experiment, by Wright *et al* (1985), illustrates further the power of the isotopic substitution method in cases where the isotopes are favourable. Dy–Ni has a eutectic point; Dy_7Ni_3 is near it and the glass can be melt spun. Figure 12.7 shows diffraction patterns taken at room temperature. In $Dy_7{}^0Ni_3$ the pattern is due to Dy–Dy distances which must also dominate the diffraction from the unsubstituted alloy because of the similarity of its pattern. Coherent neutron scattering being virtually absent from the double-null alloy, the ${}^0Dy_7{}^0Ni_3$ curve displays the magnetic scattering factor of Dy (compare figure 3.2). Magnetic ordering does not show itself at room temperature in the paramagnetic regime but peaks due to it show clearly, not only below the magnetic transition temperature of 38 ± 1 K, but also above this showing that short-range magnetic order persists up to about 150 K. More—such as inelastic scattering from the double-null alloy—can be expected from this type of investigation.

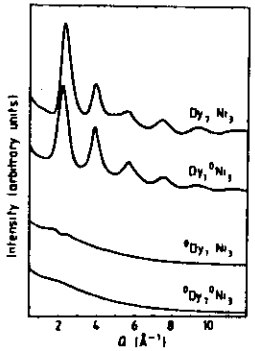

Figure 12.7 Diffraction intensity from amorphous Dy_7Ni_3 showing the use of null elements (from Wright *et al* 1984).

These three examples of diffraction and others in the literature show how important detailed studies are of the partial structure factors and how significant chemical ordering is. Hypotheses of random packing of spheres or small seeds (§2.6) are unlikely to lead to models that reproduce all the features that are emerging. Even with additional clues from EXAFS, NMR and Mössbauer experiments (Steeb and Warlimont 1985) the structural details of metallic glasses, as of other glasses, remain elusive (Cowlam and Gardner 1984).

Computer modelling was described in §2.6 and it has been applied with some success to binary metallic glasses. The $g_{ij}(r)$'s of $Fe_{80}B_{20}$, referred to above, were quite well reproduced by relaxing a DRPHS cluster of 1000 atoms using a truncated Lennard-Jones potential (Lewis and Harris in Giessen (1980), p 547). But in general the initial DRP may prejudice the outcome making the relaxation method less reliable that an *ab initio* MD simulation.

$S(Q, \omega)$, and the vibrational states of a metallic glass, were briefly discussed in §8.5 and figure 8.11, and have been reviewed by Suck and Rudin (in Beck and Güntherodt 1983). In general, the interpretation of neutron inelastic scattering from metallic glasses is not easy. For $\hbar\omega > 10$ meV there is a close resemblance between $S(Q, \omega)$ for a glass and for a polycrystalline metal of which the density and SRO are similar. As with infrared spectroscopy of non-metallic glass (§8.6), the inference seems to be that the SRO determines the main features of the thermal motion. This does not apply at $\hbar\omega < 10$ meV where there is greater intensity in the scattering from the glass which disappears on crystallisation. This implies low-energy modes which are characteristic of the amorphous structure and they may be localised and connected with the two-level system involved in low-temperature tunnelling processes (§§10.7, 12.3).

12.3 Electronic spectrum

The problems of calculating and measuring $g(E)$ and related quantities in metallic glasses have a lot in common with those in liquid metals and amorphous semiconductors, and the methods given in Chapters 7 and 11 are available. In §7.4, amorphous Fe was taken to exemplify the use of the recursion method with a cluster. Some more examples follow below. The point has been made before that the gross features of $g(E)$ are determined by the SRO; in general, the presence or absence of LRO determines the existence or sharpness of peaked details or band edges. Because of the difficulty of density of states calculations in non-periodic systems there is a tendency to find ways of keeping as close as possible to crystal calculations while incorporating some features of the SRO of the glassy state. Photoelectron spectroscopy and optical properties are obvious candidates for the experimental studies.

Before considering UPS it is interesting to enquire whether clues to $g(E_F)$ can be found in the specific heat (C) or magnetic susceptibility (χ). Neither are very illuminating. The specific heat of non-magnetic metallic glasses at low temperatures can be represented by an equation of the form used for insulating glasses (equation (10.5)) but the interpretation is not the same. Assuming the T^3-term can be understood as a Debye phonon contribution, the linear term, γT, is due mainly to the electronic specific heat and γ may be

written

$$\gamma_{obs} = \gamma_{el}(1 + \lambda_{ph}) + \gamma_{gl}. \qquad (12.1)$$

Here $\gamma_{el} = (\pi^2/3)k_B^2 g(E_F)$ and λ_{ph} is an enhancement factor from electron-phonon coupling. γ_{gl} is a contribution similar to that discussed in §10.7, for it appears that a two-level system operates to give a linear specific heat anomaly in metallic as in other glasses. However, γ_{gl}/γ_{el} might be as low as 10^{-2} so the properties of γ_{gl} are difficult to disentangle. Nevertheless γ_{gl} was discovered in glassy Zr–Pd by Graebner *et al* in 1977 and some of the other phenomena associated with two-level systems in §10.7 have also been found in metallic glasses (Black in Güntherodt and Beck (1981)). γ_{obs}/γ_{FE} varies from about 1 to about 2.5 but even if γ_{gl} is negligible, an independent value of λ_{ph} is needed to find $g(E_F)$ from γ_{obs}. λ_{ph} is referred to again in §12.5.

Similarly, it is not easy to infer $g(E_F)$ from χ. In glasses of simple metals very often $\chi < 0$ and the subtraction of the diamagnetic contribution of the ion cores leaves an electronic part which is usually significantly greater than χ_{FE} by a factor of two or more (Mizutani 1983). Part of this is presumably an enhancement due to electron–electron interactions (Nozières and Pines 1966).

In the previous section the structure of Cu–Ti was discussed. The UPS spectrum and reflectivity of a representative composition are shown in figure 12.8. By comparison with the spectra of pure polycrystals—also in figure 12.8(*a*)—and from a general knowledge of transition metal states, we infer that the peak in the glass spectrum near 3 eV consists mostly of Cu 3d states and the peak near E_F of Ti 3d states. The Drude optical formulae (§6.15) served well for NFE liquid metals in the infrared but here, with two pronounced peaks in $g(E)$, it is not surprising that the reflectivity departs radically from the Drude prediction and shows evidence of transitions upward from the peaks (figure 12.8(*b*)). The authors of this work (Lapka *et al* 1985) were able to show that if $g(E)$ is parametrised to have the form of the UPS spectrum then equation (7.43*a*) for the real part of σ, inserted into equations (6.61) and (6.62) lead via ε_R and ε_I to the observed reflectivity. They also computed $g(E)$ for a crystalline sample having the FCC structure of CuAu. As is often the case, the results were in qualitative agreement with the UPS spectrum (see figure 12.8(*a*)), quantitative agreement being too much to expect without using the real SRO of the glass.

One way of incorporating the latter while still retaining some of the relative simplicity of lattice calculations was used by Khanna *et al* (1985) for the glass Ni-P. Any use of the CPA-KKR for substitutional alloys (§7.2) or the EMA-KKR for liquid or amorphous metals (§7.3) requires the construction of muffin-tin potentials. The potential inside a muffin-tin sphere is contributed in part by the neighbours and will therefore depend on where the neighbours are. To make the point for a disordered pure metal we could write the charge density inside a muffin-tin sphere as its own density, ρ_a, plus

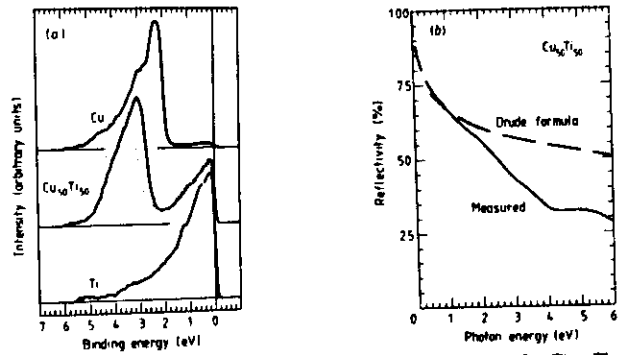

Figure 12.8 (*a*) The UPS observations on splat-cooled amorphous $Cu_{50}Ti_{50}$. The broken curve is calculated—see text. The Cu and Ti curves are for polycrystalline elements. The excitation energy was 21.2 eV. The zero of energy is E_F. (From Lapka *et al* 1985.) (*b*) Optical reflectivity of $Cu_{50}Ti_{50}$ glass.

a correction from the neighbours thus:

$$\rho(r) = \rho_a(r) + n_0 \int g(r)\rho_a(r - r')\,dr'$$

where n_0 is the number density. This could be generalised to include the $g_{ij}(r)$'s in an alloy and it makes clear that the potential depends on the SRO. This brings up yet again a problem posed by disorder: strictly every atom has a different neighbourhood and therefore a different potential, and using a mean potential derived from $g(r)$ involves the approximation of averaging at the beginning rather than at the end of the calculation. Khanna *et al* argued that the influence of SRO is more important on the potential than on the subsequent calculation of $g(E)$ and that one can therefore use the CPA instead of the more complicated EMA. It certainly appears that $g(E)$ calculated for the glass $Cu_{60}Zr_{40}$ reproduces the observed photoemission spectrum fairly well whether the EMA or CPA is used. Applying the CPA-KKR to a FCC random binary alloy of $Ni_{74}P_{26}$, with the number density of the glass, leads to figure 12.9. Experimental $g_{ij}(r)$'s were used to compute the muffin-tin potential.

$g(E)$ for the glass has many interesting features. There is the general removal of peaks characteristic of crystalline Ni and the appearance of a bulge of s states of P at -0.4 Ryd. The p states of P hybridise with Ni states to increase $g(E)$ substantially above the bottom of the pure Ni band. $g(E_F)$

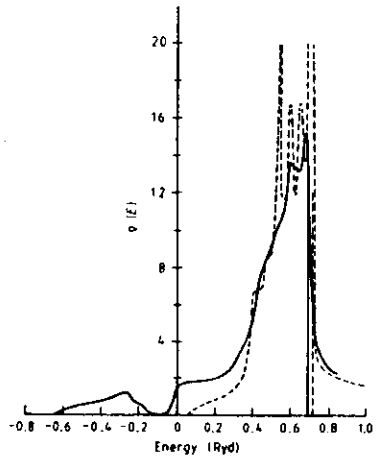

Figure 12.9 Density of states in Ni (broken curve) and $Ni_{74}P_{26}$ glass (full curve). Vertical lines indicate E_F. (After Khanna *et al* 1985.)

is reduced, but E_F remains near the top of the d band which does not fill up.

It is valuable to relate these results to various observations and to the hypothesis of Nagel and Tauc about glass formation (§12.1). E_F does not lie in a pseudogap and does not in fact change much as P enters, so there are always holes in the d band. Photoemission confirms both this and the increase in the total bandwidth. Both the Knight shift and the electronic specific heat are proportional to $g(E_F)$ and are shown by experiments to fall by factors of about two across the glass-forming range from about 15 to about 26 at .% of P. The calculation gives a decrease by about 1.4 which is much nearer to the observed factor than it would be if the P electrons simply filled up the Ni band and then pushed E_F upwards into the Ni s–p band where $g(E)$ is lower. The latter shift is what was supposed to happen on the rigid-band hypothesis with the consequence that k_F would increase with added P until $2k_F/Q_p$ in the glass-forming range as required by the Nagel and Tauc hypothesis. Although this appears not to happen, the extension of the s–p band downwards relative to the d band has the same effect of increasing k_F (Khanna *et al* 1985).

A number of other methods have been tried for calculating $g(E)$ in alloy

glasses. Several are in *Proc. 5th Int. Conf. on Liquid and Amorphous Metals* (1984) which also contains a review by Cyrot-Lackman. We refer to one other example: Fujiwara's calculation for Fe–P and Fe–B, which are both much studied glass-forming alloys (Fujiwara 1983).

The muffin-tin concept is used again but this time the structure is given by a relaxed DRP model of about 1500 spheres with diameters adjusted to give RDF in agreement with the observed ones. Inside a Wigner–Seitz cell in a crystal it is possible to conceive electron wavefunctions made up by linear superposition of muffin-tin orbitals derived from the cell, and from all its neighbours, in such a way that the sum is a solution of Schrödinger's equation inside the cell. This can be implemented numerically and works well in band structure calculations in crystals. On replacing the Wigner–Seitz cell with a sphere of the same volume, a simplification results; and by distributing the spheres according to the DRP model the method becomes applicable to glasses. The actual computation is performed by the recursion technique

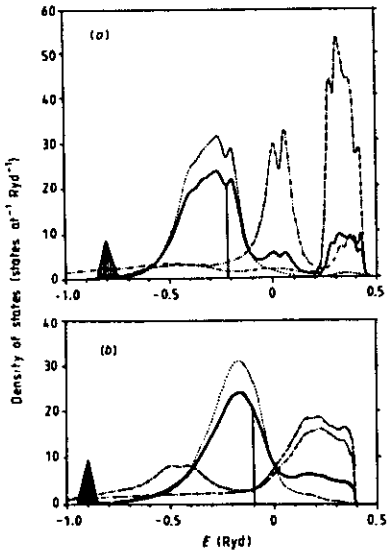

Figure 12.10 $g(E)$ in (*a*) $Fe_{75.2}B_{24.8}$ and (*b*) $Fe_{75.7}P_{24.3}$. Full curve, the glass; dotted curve, Fe 3d states; ···–···, Fe 4s states; chain curve, P 3p or B 2p states. The shaded triangle shows the position and weight of P 3s and B 2s states. (From Fujiwara 1983.)

(§7.4) and the details are given in Fujiwara (1983). The results have much in common with those quoted above for Ni-P. Figure 12.10 shows how the B or P s states appear at the low end of a broadened density of states. E_F remains near the top of the d band and in both Fe-B and Fe-P, $g(E_F)$ falls as the non-metal is added. The $g(E)$ is in qualitative agreement with UPS and XPS spectra.

These examples show that, in metallic glasses as in liquid metals and amorphous semiconductors, density of states calculations have become reasonably reliable and realistic in spite of the simplifications which are inevitable for modelling the structure and for making the computation tractable.

12.4 Electron transport properties I: simple metal alloys

Suppose that in the absence of experimental results a theory was required to predict the resistivity, $\rho(T)$, at constant volume, of an amorphous metallic element. In a pure perfect crystal the resistivity is known to derive from the electron-phonon interaction: scattering from the ions in their lattice positions is ignored because it leads to Bragg reflections and the band structure, not to resistance. This means that only the vibrational part of the dynamic structure factor is used for calculating the electron scattering, the part leading to Bragg scattering being subtracted out; thus the resistance vanishes at absolute zero. This does not make a good starting point for an amorphous metal because the topological disorder must involve scattering even if, as at 0 K, there are no thermal vibrations. In §6.12 the Ziman theory of resistance in liquid metals was set out. This uses the static structure factor, $S(Q)$, which certainly takes the topological disorder into account but also seems unsuitable for the present purpose because phonons would presumably play some part in the resistance of an amorphous metal. In §6.16 it was pointed out that Ziman's formula is actually the high-temperature limit of a more general theory in which $S(Q)$ is replaced by

$$S^{\alpha}(Q) \equiv \int_{-\infty}^{+\infty} S(Q,\omega)\frac{\hbar\omega}{k_B T} n(\omega)\,d\omega \qquad (12.2a)$$

where

$$n(\omega) \equiv [\exp(\hbar\omega/k_B T) - 1]^{-1}.$$

This means that from equation (6.59)

$$\rho = \frac{3\pi}{e^2 k_F^2}\left(\frac{N}{V}\right)\langle\langle S^{\alpha}(Q)|w(Q)|^2\rangle\rangle. \qquad (12.2b)$$

$S^{\alpha}(Q)$ is sometimes called the resistivity structure factor and includes both the static topological disorder and the vibrations; it looks the appropriate

quantity for glassy metal resistance. Even so generalised, the NFE theory is only a diffraction theory suitable for weak scattering or low-resitivity systems and would probably only apply, if at all, to glasses of simple metals. Further, the partial resistivity structure factors, $S^{\alpha}_{ij}(Q)$, would be required for alloys where chemical, as well as topological, disorder prevails.

This poses very formidable theoretical problems. The calculation of $g(Q,\omega)$ from first principles were referred to in §8.5 where an example was given to show that it can be done. But a number of theories of resistivity have been published which avoid having to do this by adopting approximations for $S^{\alpha}_{ij}(Q)$. These result from simplifying assumptions about $S(Q,\omega)$, namely, that it represents plane-wave phonon propagation with a linear dispersion law like sound waves; or, alternatively, that every atom vibrates independently. These represent the extremes of coherent and incoherent thermal motion (see, e.g., §8.3). A detailed derivation of these approximate $S^{\alpha}_{ij}(Q)$'s will not be made here but they will be quoted to show what they, and consequently the resistance, depend on.

Before doing this we should pause to ask if it is reasonable to expect a NFE theory to apply to metallic glasses at all. With liquid metals we saw that one source of confidence was the free-electron value of R_H (§6.14), but that this could not always be relied on even for seemingly simple alloys. The matter has been quite thoroughly investigated for binary and ternary glasses of simple metals and it appears that $R_H \simeq R_H^{FE}$ in very many cases although, as might be expected from §6.14, not with Bi–Pb alloys (Mizutani 1983). Save for such exceptions, $2k_F$ may be inferred from $2k_F = 1.139 \times 10^{-3}(-R_H)^{-1/3}$ Å^{-1} where R_H is in m^3 A^{-1} s^{-1}. $2k_F$ is of course an important input to the generalised Ziman theory. Alloys with $R_H \simeq R_H^{FE}$ are also of relatively low resistivity on the whole.

Returning now to $S(Q,\omega)$ and $S^{\alpha}(Q)$ we quote from the work of Jäckle and Frobose via that of Hafner and Philipp (1984). For the plane-wave model of $S(Q,\omega)$, and in the case that one-phonon processes are adequate,

$$S^{\alpha}_{ij}(Q) = \exp[-(W_i + W_j)]\Big[S^{(AL)}_{ij}(Q) + \frac{\hbar^2 Q^2}{k_B T (M_i M_j)^{1/2}} \times \Big(c_s n(c_s Q)(n(c_s Q)+1) + \frac{1}{(2\pi)^3 n_0} \times \int n(c_s k)(n(c_s k)+1) S^{(AL)}_{ij}(k+Q)\,d^3k\Big)\Big] \qquad (12.3a)$$

where M_i is the ion mass, c_s is the sound velocity and n_0 is the mean ion number density. In this expression, $\exp(-W_i)$ is the Debye–Waller factor for type-i atoms. This factor determines the reduction in intensity of Bragg peaks due to thermal vibrations during x-ray diffraction from a crystal, and reappears here in the one-phonon scattering of electrons (Ashcroft and Mer-

min 1976). W_i is a function of T and Q, namely,

$$W_i(Q, T) = \frac{\hbar^2 Q^2}{2M_i} \int_0^{\omega} \omega^{-1} g_i(\omega)(n(\omega) + \tfrac{1}{2})\, d\omega \qquad (12.3b)$$

where $g_i(\omega)$ is the partial density of vibrational states. We note further that the static partial structure factors have been given the Ashcroft–Langreth form of equation (3.36). The sound velocity is assumed to be the same for both longitudinal and transverse modes—a simplifying assumption to help evaluate $S(Q, \omega)$.

For the incoherent vibration model,

$$S_{ij}^{\text{in}}(Q) = \exp[-(W_i + W_j)]\left(S_{ij}^{(\text{AL})}(Q) + \frac{\hbar^2 Q^2 \delta_{ij}}{2k_B T (M_i M_j)^{1/2}} \times \int_0^{\omega} n(\omega)(n(\omega) + 1) g_i(\omega)\, d\omega\right). \qquad (12.3c)$$

Equations (12.2) and (12.3) enable $\rho(T)$ to be calculated if the $S_{ij}^{(\text{AL})}(Q)$ and $u_i(Q)$ are known. The $u_i(Q)$ are chosen from pseudopotential theory and lead to ion–ion potentials (§6.7). The latter can be used to determine the equilibrium density and the $S_{ij}^{(\text{AL})}(Q)$ by a cluster relaxation method like that outlined in §8.5. The $g_i(\omega)$ are also required and the recursion method is available for this. This somewhat formidable programme of calculation has been carried out for $Ca_{70}Mg_{30}$ (Hafner and Philipp 1984) and for $Mg_{70}Zn_{30}$ (Hafner 1985). It amounts to a calculation of ρ from first principles and some results are given in table 12.2 and figure 12.11.

Table 12.2 Residual resistivities ($\mu\Omega$ cm).

	Experimental	Theoretical
$Ca_{70}Mg_{30}$	43.7	35.6
$Mg_{70}Zn_{30}$	43 to 57	43.6

The diagrams illustrate several points of general interest. First, the temperature coefficient of resistance (TCR) is positive in one and negative in the other. Liquid Zn also has a negative TCR and an explanation was given in §6.13 in terms of the proximity of $2k_F$ to Q_p, and the temperature variation of the static structure factor. This kind of explanation is still available from the first term of equation (12.3). But the second or phonon term gives a positive TCR. In $Ca_{70}Mg_{30}$ the latter dominates and in $Mg_{70}Zn_{30}$ the former does. This can be shown in detail by examining the Q- and T-dependences of the factors in the integrand of equation (12.2b). It is clear that with three or more S_{ij}'s and two or more pseudopotentials and $g_i(\omega)$'s, there is scope for

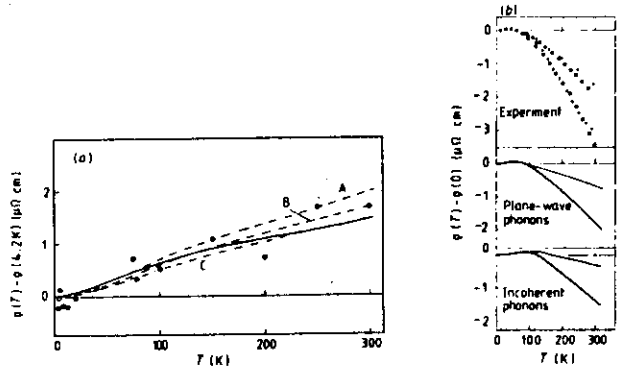

Figure 12.11 Experimental and calculated resistivities for: (*a*), $Ca_{70}Mg_{30}$; (*b*), $Mg_{70}Zn_{30}$. In (*a*) the full curve is theoretical and the points experimental; the broken curves show the effect of different Debye temperatures (A, 230 K; B, 250 K; C, 270 K). In (*b*) the thin line is isochoric and the thick line isobaric. The observed points are from four different experiments. (After Hafner and Philipp (1984) and Hafner (1985). For more detail, see these papers.)

much detailed behaviour and variation from glass to glass. This is further shown by the ability of the theory to reproduce the maxima and minima in ρ that are observed for $T < 60$ K in $Mg_{70}Zn_{30}$ (Hafner 1985).

$(\partial\rho/\partial T)_v$ and $(\partial\rho/\partial T)_p$ are different. The difference is not always great but is measurable in, say, liquid alkali metals near their melting points and is enormous in the expanded liquid metals of §11.12. Experiments are usually done at constant pressure so the theory should allow for thermal expansion. This is done in figure 12.11(*b*) and is obviously necessary.

Calculations of this type are no doubt improving but it seems clear that the generalised Faber–Ziman theory is quite capable of explaining $\rho(T)$ in glassy alloys of simple metals if pursued with sufficient attention to all the inputs to the equation. The negative TCR of $Mg_{70}Zn_{30}$ is by no means unusual, indeed dozens of simple metal glasses have it and in most cases $2k_F/Q_p \simeq 1$, strongly suggesting that the first term of equation (12.3) is dominating the temperature dependence giving an effect similar to that in divalent liquid metals (Mizutani 1983).

Although the NFE theory provides a formula for the thermoelectric power (§6.12), it is difficult to fit it to the data. This is partly because of the sensitivity of the theoretical value to the ~~values of~~ $u_i(2k_F)$ and $S_i(2k_F)$ ~~which are uncertain~~ and also possibly to electron–phonon enhancement effects not

included in the theory (see below). In the accumulated data, both positive and negative α's and $d\alpha/dT$'s are found (Mizutani 1983).

12.5 Electron transport properties II: non-simple cases

The two simple glasses mentioned above and a large number of others have ρ at 300 K well below 100 $\mu\Omega$ cm. Many other glasses containing non-simple metals have much higher resistivities and are consistent with interesting generalisations made by Mooij (1973). One of these says that the TCR correlates strongly with $\rho(300)$, being positive for $\rho(300) \leqslant 150\ \mu\Omega$ cm and negative for higher ρ's. This applies to crystalline or amorphouse alloys and to liquids, with few exceptions. The other Mooij generalisation is that, irrespective of the low-temperature resistivity, alloys tend at high temperature towards a saturation value of $\rho \sim 150\ \mu\Omega$ cm. Some evidence bearing on this point is shown in figure 12.12.

To see that considering non-simple metals means relinquishing the NFE model, we have only to look at R_H which is sometimes positive and is, in any case, hard to compare with a free-electron value because of the difficulty of saying how many electrons are 'free'. An example is the Hall effect in melt-spun Cu–Zr, studied by Gallagher *et al* (1983). The resistivity at 300 K is typically about 180 $\mu\Omega$ cm and the TCR negative. Ageing the samples over many months greatly alters the TCR and R_H, apparently because of progressive surface oxidation leading to crystallisation. The reproducible results from new samples are added to others on liquid alloys from Künzi and Güntherodt (1980) in figure 12.13. Pure Cu has $R_H = R_H^{FE}$ but the sign change occurs at about 20 at. % of transition or rare-earth metal. R_H in Cu–Zr varies very little with temperature from 0 to about 250 K which is normal.

$R_H > 0$ remains hard to account for however. The need is for acceptable, preferably rigorous, expressions for σ_{xx} and $\sigma_{xy}(H)$ in equation (7.46), and a way of evaluating them with wavefunctions which are hybrids of s and d states in alloys containing transition metals. Both of these requirements seem not to have emerged fully from the formative stage at the time of writing but, given certain assumptions plausible for glasses, Morgan and collaborators have argued that R_H depends only on electron properties at E_F, that

$$R_H \propto (\mathrm{d}g(E)/\mathrm{d}E)_{E_F},$$

and that the latter can give $R_H > 0$ in regions of anomalous dispersion where $(\partial E/\partial k) < 0$ (see figure 7.5). On this basis R_H and σ can be computed reasonably well for CuZr alloys (Morgan and Howson 1985, Howson and Morgan 1985, Nguyen-Manh *et al* 1986).

To explain the existence of high resistivities some application of the Kubo equations will surely to be required. In §7.7 it was pointed out that a Kubo

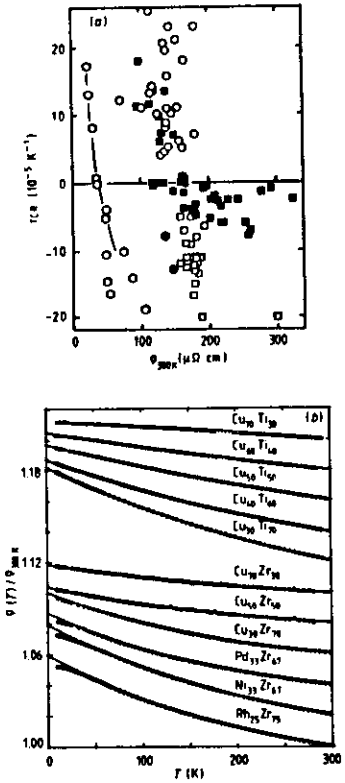

Figure 12.12 (*a*) Correlations of TCR with resistivity at 300 K. ○, ferromagnetic; ■, metal/metalloid alloys (paramagnetic); □, metal–metal alloys (paramagnetic); ⊗,○, weakly paramagnetic or diamagnetic with/without $\rho \propto (1 - AT^2)$ at low T. (*b*) Examples of negative TCR in N–T and T–T alloys. The curves are vertically displaced by 0.02. (After Mizutani in Steeb and Warlimont (1985). For more detail see Mizutani (1983).)

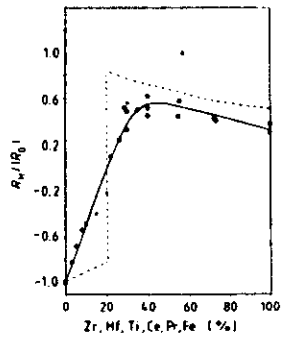

Figure 12.13 Onset of positive Hall coefficients in disordered alloys. ●, Cu–Zr; ■, Cu–Hf; ▲, Cu–Ti; ○, Cu–Ce (liq); □, Cu–Pr (liq); △, Ag–Pr (liq); +, Au–Fe (liq). (From Gallagher *et al* 1983.)

formula for diffusivity, applied to a cluster, had been successfully used with the recursion method to calculate ρ in disordered Fe. In fact a good account of ρ in liquid V, Cr, Mn, Fe, Co and Ni (mostly $\rho > 100\ \mu\Omega$ cm) has been given by this method and there is no reason in principle why it should not be used for amorphous metals (Ballentine 1985). It would be valuable in addition to have an argument which—like the NFE model in its context—gives some intuitive understanding of how small or negative temperature coefficients of resistance can arise in high-resistance amorphous alloys, and some work by Schirmacher and colleagues is interesting in this respect. Using arguments for which the original papers must be consulted, Belitz and Schirmacher inferred from the Kubo formulae that

$$\sigma = e^2\left(\frac{n/m}{M_0 + M_T} + L_0 + L_T\right).$$

The M-terms show σ controlled by scattering and the L-terms represent σ enhanced by hopping or tunnelling. The suffix 0 refers to elastic scattering or to tunnelling processes subject to static disorder; the suffix T is for inelastic scattering and tunnelling enhanced by dynamic disorder. The latter includes both coherent or phonon modes and incoherent or diffusive motion (Schirmacher 1985). In the expressions for the M's and L's it is not surprising to find $S(Q)$ and $S''(Q)$ in the static and dynamic parts. The behaviour depends on the relative sizes of the terms. For metals of low resistivity the formula reduces to equation 12.2(h), but for more disorder and stronger interactions when the mean-free path is comparable with the de Broglie wavelength

$2\pi/k_F$, the L-terms begin to take effect and can give a conductivity which is enhanced by thermal motion leading to an overall negative TCR. The substantial amount of structural and dynamic input data needed for applying the theory to a real alloy is rarely, if ever, available.

The thermoelectric power usually requires careful interpretation and it was soon suspected that equation (6.49) for the diffusion thermopower was inadequate for amorphous alloys. We rewrite it here as

$$\frac{\alpha_{th}}{T} = \frac{-\pi^2 k_B^2}{3|e|E_F}\xi \qquad \xi \equiv \left(\frac{\partial \ln \sigma(E)}{\partial \ln E}\right)_{E_F}. \tag{12.4}$$

One correction that need *not* be applied is for phonon drag. This arises from the non-equilibrium phonon distribution, or streaming by phonons in a temperature gradient, which is important in crystals but may be ignored in glasses because the disorder scatters phonons strongly and keeps them essentially in equilibrium (Jäckle 1980). Electron–phonon interaction is important nonetheless because it requires electrons to be treated as quasiparticles with effective mass m^* such that $m^*/m = 1 + \lambda_{ph}(T)$ where $\lambda_{ph}(T)$ is called the mass enhancement and depends on the electron-phonon coupling constant. This does not affect the conductivity but its energy dependence multiplies ξ by $1 + \lambda_{ph}(T)$ (Jäckle 1980).

The suggestion that $\lambda_{ph}(T)$ was important for metallic glasses was taken up experimentally by Gallagher and theoretically by Kaiser in 1981. ~~His~~ Some experimental results for Cu–Zr, Cu–Ti and other alloys had the form shown in figure 12.14 which is from later work (Gallagher and Hickey 1985, see also Kaiser 1982). The argument was that ξ should vary very little, if at all, with temperature because magnetic scattering was absent, and because the small TCR ~~counteracted~~ counteracting any large changes with temperature in the relative importance of s and d electron contributions, or of competing scattering mechanisms. The observed failure of α/T to remain constant below about 200 K was therefore assigned to $\lambda_{ph}(T)$. The phenomenon has since been detected in many more glasses and the explanation essentially confirmed, though not without further examination which revealed several more corrections. For example, α_{th} should be replaced by $\alpha_{th}(1 + AT^{1/2})$ because of electron–electron interactions; $\lambda_{ph}(T)$ should be given a constant increment λ_{sf} due to spin fluctuations; and α/T acquires an increment due to the effect of electron–phonon interactions on electron velocities and relaxation times—an effect not included in m^*. Altogether

$$\frac{\alpha}{T} = \frac{\alpha_{th}}{T}(1 + AT^{1/2})(1 + \lambda_{ph}(T) + \lambda_{sf}) + (2\gamma_1 + \gamma_2)\lambda_{ph}(T)$$

where λ_{sf} and the constants γ_1, γ_2 are given by the theories. It appears however that the $AT^{1/2}$ and λ_{sf} terms have very little influence and that the observed λ_{ph} ($T = 0$), about 0.4 to 1.0, agree well with those obtained independently from superconducting transition temperatures (Gallagher and

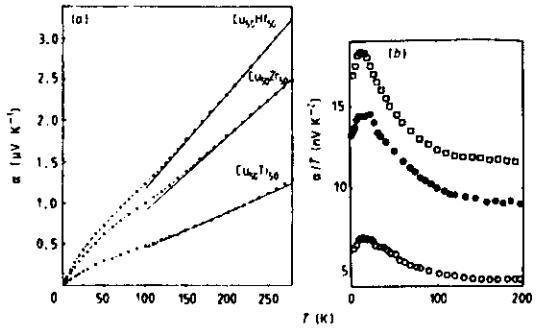

Figure 12.14 α and α/T in three glasses (from Gallagher and Hickey 1985).

Hickey 1985, Kaiser 1982). It remains a problem whether the observed $\lambda_{ph}(T)$ agrees with the theory of electron–phonon interaction which involves a coupling constant of uncertain frequency dependence (Sato *et al* 1986).

There is still the question of the absolute value of ξ, for which a theory of $\sigma(E)$ is needed. Equations (6.60) from the NFE theory, or, for transition metals, its extended version (§6.16), are a possibility. Or, in a theory of Mott in which current is carried by s and p electrons but limited by scattering into empty d-band states, ξ depends on $(\mathrm{d} \ln g(E)/\mathrm{d} \ln E)_{E_F}$ and its sign therefore varies with that of $(\mathrm{d}\, g(E)/\mathrm{d}E)_{E_F}$. Neither of these models fit all the facts, and the extended Ziman theory certainly looks unsuited to non-simple glassy alloys. Since there is evidence for substantial current carrying by d electrons in some metals (§7.7) a full theory of α should include (Gallagher and Greig 1982).

In §7.7, '$2k_F$ scattering' was introduced and §9.11 brought a logarithmic temperature dependence of conductivity into the weak localisation regime in 2-D. Since about 1980 these ideas have been imported into the theory of high-resistivity metallic glasses of which the negative TCR has presented a puzzle. This is an alternative approach to the one above by Schirmacher and Belitz and the relation between the two methods is not altogether clear. For simplicity let us assume that in the absence of $2k_F$ scattering, the conductivity would have the Boltzmann value, equation (6.52), which can easily be manipulated to read

$$\sigma_B(T) = \sigma_B(0) + \sigma_B^{(T)} = \frac{1}{3\pi^2}\left(\frac{e^2}{\hbar}\right)(k_F l_e)^2\left(\frac{1}{l_e} - \frac{1}{l_i(T)}\right) \qquad (12.5)$$

Here, l_e and $l_i(T)$ are the elastic and inelastic mean-free paths as in §9.11.

$\mathrm{d}\sigma_B(T)/\mathrm{d}T$ is always negative because $l_i(T)$ falls with rising T. A correction would be necessary if the scattering were so great that $g(E_F)$ was seriously affected but we ignore this (Mott and Kaveh 1985).

A regime in which $2k_F$ scattering is present, but is not sufficient to cause localisation, is sometimes said to show 'localisation effects' or 'incipient localisation'. The theory in 2-D leads to equation (9.18) and, in 3-D, σ_B is corrected to $\sigma_B(T) + \sigma_L(T) = \sigma_B(T) + \sigma_L(0) + \sigma_L^{(T)}$. The correction σ_L is obtainable either from a multiple-scattering calculation (Kawabata 1982, see also Lee and Ramakrishnan 1985) or from a method in which electron wavefunctions, believed to combine components both extended and decreasing with a power law, are related to electron diffusion and then used in the Kubo-Greenwood equation of §7.7 (Mott and Kaveh 1985). In either case the formulae are

$$\sigma_L(0) = \frac{-C\sigma_B(0)}{(k_F l_e)^2} = \frac{-C}{3\pi^2}\left(\frac{e^2}{\hbar}\right)\frac{1}{l_e} \qquad (12.6a)$$

$$\sigma_L^{(T)} = \frac{-C\sigma_B^{(T)}}{(k_F l_e)^2} + \frac{C\sigma_B l_e}{(k_F l_e)^2 L_i(T)} \simeq \frac{C}{3\pi^2}\left(\frac{e^2}{\hbar}\right)\frac{1}{L_i(T)} \qquad (12.6b)$$

where $L_i(T) \simeq (l_i(T) l_e)^{1/2}$, the inelastic diffusion length (see also §9.11), and C is a constant of order unity. The last approximation uses $l_e \ll l_i$ and $L_i \ll l_\varphi$, which are reasonable in disordered glasses.

Concentrating on the temperature-dependent part, $\sigma_B^{(T)} + \sigma_L^{(T)}$, we see it is approximately

$$\frac{1}{3\pi^2}\left(\frac{e^2}{\hbar}\right)\left(\frac{C}{L_i(T)} - \frac{(k_F l_e)^2}{l_i}\right)$$

and in high-resistivity glasses where l_e is very small—perhaps only about a nearest-neighbour distance—only the first term matters.

In connection with the first relevant experiments in glasses, Howson pointed out that the temperature dependence of σ would therefore depend on that of $l_i(T)$. Electron–phonon scattering is dominant and the theory of this shows that $l_i(T) \propto T^{-2}$, whence $\sigma \propto T$ for $T < \theta_D$; and $l_i(T) \propto T^{-1}$ whence $\sigma \propto T^{1/2}$ for $T > \theta_D$. Both give a negative TCR. This has been confirmed experimentally for a number of glasses—see figure 12.15.

As with localisation in 2-D (§§9.11, 9.12), the incipient localisation in 3-D can be affected by electron–electron interactions. There seems not to be an intuitive and transparent way of seeing what the effect is. Detailed calculations show that $g(E)$ is altered, up or down, by a correction proportional to $|E - E_F|^{1/2}$ and that a consequence is that σ is corrected by a term propor-

tional to $T^{1/2}$. This term can be written (Al'tshuler and Aronov 1979)

$$\sigma_1 \simeq \frac{1.3e^2}{4\pi^2\hbar}\left(\tfrac{4}{3}-\tfrac{3}{2}\tilde{F}\right)\left(\frac{k_B T}{2\hbar D}\right)^{1/2} \qquad (12.7)$$

where the suffix I indicates 'interaction', D is the electron diffusion coefficient and $\tilde{F}$ was introduced in §9.11.

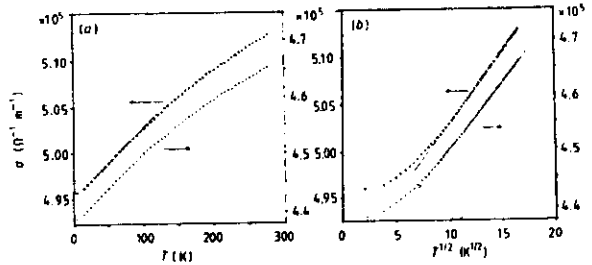

Figure 12.15 Temperature variation of σ in $Ti_{50}Be_{40}Zr_{10}$ (×) and $Cu_{50}Ti_{50}$ (●) glasses, showing the T- and $T^{1/2}$-dependences (from Howson 1984).

This effect is distinct from the $T^{1/2}$-dependence in σ_L and has been detected *below* the linear region of σ_L, say at $T \leqslant 10$ K. Figure 12.16 shows this and, as T rises from a few K to about 300 K, regimes of $T^{1/2}$, T- and $T^{1/2}$-dependences succeed each other and conductivity extrema may well separate the regimes, giving a complex temperature dependence overall (Cochrane and Strom-Olsen 1984, Howson and Greig 1984).

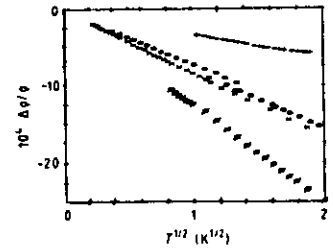

Figure 12.16 $T^{1/2}$-dependence of ρ at low temperatures (from Cochrane and Strom-Olsen 1984).

Recalling §9.11 again, we expect a magnetic field to produce complex effects in σ. There are at least four sources of this: cyclotron orbits introduce a new length into the problem and affect localisation thereby; the orbits, and also the Zeeman splitting of spin states, affect the electron-electron interaction term; these are the effects symbolised by the $\Delta\sigma(H)$ terms in equation (9.20). The spin-orbit (so) interaction must also be allowed for and, in addition, if the material is superconducting, fluctuations in its thermodynamic variables, occurring at $T \sim T_c$, cause observable changes in electron transport (and other) properties (Skocpol and Tinkham 1975) which can be further modified by the magnetic field. By choosing appropriate samples, one or more of these effects can be virtually eliminated and a magnetoresistance experiment used to check the others. Thus Bieri *et al* (1984) observed positive magnetoresistance in $Cu_{57}Zr_{43}$ glass and interpreted it as the effect of H on localisation and superconductivity fluctuations. Poon *et al* (1985) show that a similar property exists in Lu-based glasses and argue that it is almost entirely due to the effect of H on localisation, superconductivity being absent and other sources largely eliminated by a high spin–orbit effect.

As first suggested by Howson and Greig (1983), the magnetoresistance in alloy glasses is a valuable indicator of localisation and interaction effects in 3-D. There are considerable difficulties in both experiment (quite small $\Delta\sigma(H)$ at very low T) and theory (many effects interfering with each other). Nevertheless at the time of writing valuable progress is elucidating not only the properties of metallic glasses but *ipso facto* the general phenomena of localisation and interaction characteristic of many disordered systems (Hickey *et al* 1986).

In this and the previous section, the electron transport properties of metallic glasses have been illustrated by examples. There are many more. In particular, magnetic impurities and ferromagentism cause characteristic phenomena like the Kondo effect and the anomalous Hall effect but these will not be pursued here (See, e.g., Luborsky 1983).

12.6 Other important properties

The object of this final section is to draw the reader's attention to a few important properties that the chapter does not deal with. There is a growing number of comprehensive ~~reviews~~ on metallic glasses where these subjects can be pursued (Beck and Güntherodt 1983, Luborsky 1983, Moorjani and Coey 1984, Egami 1984).

Probably the most important omitted property is the magnetism of those alloys containing transition and rare earth elements. Its importance partly derives from the technical value of the glasses, especially magnetically soft ones, for applications which include transformer cores, shielding and recording devices. Apart from this, the already profound problems of magnetism in

crystals are intensified by disorder except that those arising from an isotropy are largely removed.

The itinerant electron model of the overall average properties of ferromagnets, such as saturation magnetisation, Curie temperature and spin wave dispersion, requires a knowledge of electronic quantities including $g(E)$, the bandwidth and the electron–electron interaction energy of two electrons. Calculations such as those of §12.3 are therefore pertinent and disorder will alter the magnetic properties as a consequence of smoothing the structure of $g(E)$ without changing the behaviour in principle. But it is rarely, if ever, possible to compare directly crystalline and amorphous forms of a ferromagnetic element and the process of alloying to form a glass–such as introducing B into Fe–itself alters the magnetism by electronic changes such as hybridisation and charge transfer between impurity and host. If crystalline and glassy alloys with similar composition and SRO can be compared, however, the disorder does not normally affect the ferromagnetism radically.

This is not in general true for other forms of magnetic order. Where the lowest energy of a pair of moments is achieved by antiparallel alignment (antiferromagnetism), a ring of interacting moments will be frustrated in the attempt to realise consistent antiparallelism if the ring is odd-numbered. Frustration also occurs when two or more neighbours of one atom with antiferromagnetic coupling are also neighbours of each other; the simplest case is the triangular lattice in 2-D. Topological disorder might create such situations and profoundly alter the energetics. Topological disorder is not a necessary condition for frustration however: it can occur in the square Ising lattice when there is random mixture of ferromagnetic and antiferromagnetic couplings, with or without a random dilution of magnetic sites by non-magnetic ones; it is impossible then to satisfy simultaneously all the competing coupling requirements and the ground-state energy rises over that of an ordered system. This is a rich source of highly interesting and challenging problems in magnetism.

It is difficult to pursue such questions without a preliminary account of magnetic theory in general and, for this reason, the reader will probably want to enter the very large literature through references already quoted above. From a valuable reference (Moorjani and Coey 1984) we take pictorial illustrations of magnetic ordering possibilities in topologically disordered arrays of local moments. The distinction between figures 12.17(*a*) and (*b*) is between systems with one kind of atom with a specified moment and magnetic interaction and systems with two kinds. To these we add in figure 12.17(*c*) a sequence of possibilities opened up as the atomic percentage of random magnetic impurities increases in a non-magnetic crystal lattice. The magnetic couplings are the various forms of exchange interaction which include the direct one, which was the original explanation ferromagnetic couplings of spins, and the indirect one of Rudermann–Kittel–Kasuya–Yoshida (RKKY). In the latter, the electron gas, magnetically polarised by

the moment of one ion, transmits the magnetic effect to a distant ion through an interaction which falls off as r^{-3} and oscillates in sign with wavelength $2\pi/2k_F$. The sign oscillations imply different couplings between pairs of different separations and can be a source of frustration in disordered arrays of moments. In the spin glass regime this results in the freezing-in of moments with disordered orientation at low temperatures. Spin glasses remain an intense focus of scientific interest (Chowdhury 1986).

Like the magnetic properties, but to a lesser extent, the mechanical properties of amorphous metals have also promised practical applications: they are possible constituents of strong composite structural materials for exam-

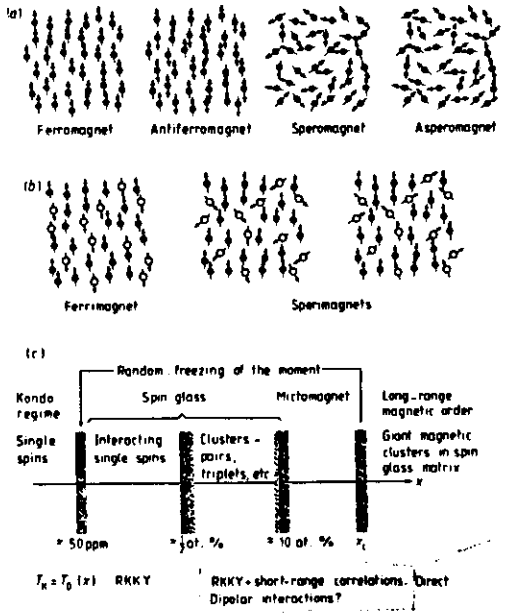

Figure 12.17 (*a*), (*b*) Schematic diagrams of various orientational ordering possibilities. Prefixes spero, speri, refer to random orientation systems with net magnetic moments. Asperomagnets have no net moment. (*c*) Various regimes at different magnetic impurity concentrations, x. The dominant interactions are shown below the diagram. x_c is the percolation threshold, e.g. about 15.5 at. % Fe in Au, at which direct interactions link up throughout the system. (After Moorjani and Coey 1984.)

ple. Their nature as glasses out of thermodynamic equilibrium complicates their mechanical properties both in theory and experiment. However, unless magnetisation and magnetoelastic effect intervene, the elasticity of metallic glasses is in general isotropic and there are only two independent properties, say the bulk and shear moduli. The former (K) is similar to, the latter (G) is about 30 % lower than in the crystalline form. At least for simple metals, an equation of state ought to be derivable from the pseudopotential theory of ion–ion interactions in which the total energy, E, has volume and structure-dependent terms (§6.6). The bulk modulus is proportional to $d^2E/d\varepsilon^2$, where ε is the strain, and it was calculated successfully in this way for amorphous $Mg_{70}Zn_{30}$ by Hafner (see Suzuki (1982), p 1311). For shear strain at constant volume, a computation of $d^2E/d\varepsilon^2$ was originally performed by Weaire *et al* (1971) using pair potentials in a model glass of about 100 atoms. It appeared that the shear modulus was reduced relative to its value in the crystal by the adjustments of configuration to which the glass can resort in order partially its shear stress.

Of course there is a great variety of responses to stress (σ_{ij}) that metallic glasses can show. The elastic response which is virtually instantaneous is homogeneous and, if the stress is prolonged and also low (say $\sigma_{ij}/G < 0.01$), homogeneous creep can be detected. For sufficiently low stress the Newtonian viscosity, $\eta = \sigma_{ij}/\dot{\varepsilon}$, can be measured and it falls as the temperature rises. More complicated stress–strain relations occur at higher stresses (see, e.g., Spaepen and Taub in Luborsky (1983)).

Flow is not necessarily homogeneous. At high stresses (say $\sigma_{ij}/G > 0.02$), glasses subjected to tensile testing or cold working show local plastic deformations. In a tensile test the latter occur in thin shear bands making an angle with the direction of tensile force and the bands are detectable at the surface. They are the sites of very large strains leading ultimately to fracture. Metallic glasses do not in general show work hardening. This inhomogeneous behaviour is not very sensitive to temperature (Luborsky 1983). In crystal physics it would be natural to discuss plastic flow in terms of dislocations. It is obvious that dislocations defined by displacement of planes of atoms are not appropriate to a glass, but not obvious that the dislocation concept it therefore of no use at all. In crystals, dislocations are associated with characteristic stress distributions and similar ones could be notionally introduced into a glass by the kind of cuts and displacements shown in figure 2.9. This has been done in computer simulations but it is not established that mobile line defects play any role in plastic flow comparable with that in crystals (Beck and Güntherodt 1983, Luborsky 1983). Metallic glasses can show strengths up to the ideal limit set by the cohesive forces.

It was mentioned earlier that structural relaxation occurs during annealing or ageing. This affects all the properties and particularly some of the mechanical ones. For a rational investigation of the temperature dependence of some property P it is desirable that the structure should remain the same,

statistically at least, during the measurements. It is found that P changes with time, t, during annealing but that $|P^{-1}dP/dt|$ gradually decreases. If P reaches a value P_0 at t_0 and temperature T_0, and thereafter changes by only a few per cent per day, it is possible to reduce T_0 to T_1 for an interval τ during which $P(T_1)$ is measured. If P_0 is regained on returning to T_0, it indicates that the structure did not change significantly during τ. This could be repeated for T_2, T_3, ..., and $P(T)$ is then attributable to a particular structure and the measurement is said to be isoconfigurational. This is a means of effectively evading the relaxation effects in order to separate the variables.

But the relaxation phenomenon is of great interest in its own right, viscosity and diffusion being particularly sensitive to it. Atomic diffusion, like plastic flow, is not so easy to envisage in glasses as in crystals because the vacancy and its jumps are not well defined. Interstitial jumping of small atoms, notably hydrogen, occur in metallic glasses, but whatever the diffusion mechanisms of large atoms are, the diffusion coefficient generally obeys the Arrhenius law $D = D_0 \exp(-Q/T)$. Since Q does not depend on T, it seems that there is not a large spread of activation energies, and therefore presumably not a large variety of displacive motions, in spite of the fact that no two jumping environments are identical (see, e.g., Cantor in Steeb and Warlimont 1985). At the time of writing it is probably true to say that the atomic mechanisms involved in the relaxation process are not well enough understood to relate the relaxation of one property with that of another.

'At the time of writing' is a phrase used not simply in relation to metallic glasses but quite often throughout the book—which may therefore reasonably be concluded by the remark that, although much of the text has dealt with well established or fundamental ideas, some of it has presaged future developments in which the reader may well be taking part.

References

Al'tshuler B L and Aronov A C 1979 *Sov. Phys.–JETP* **50** 968
Aschroft N W and Mermin N D 1976 *Solid State Physics* (New York: Holt, Rinehard and Winston)
Ballentine L E 1985 *Proc. 5th Int. Conf. on Rapidly Quenched Metals* ed S Steeb and H Warlimont (Amsterdam: North-Holland) p 981
Ballentine L E and Kolář M 1986 *J. Phys. C: Solid State Phys.* **19** 981
Beck H and Güntherodt H-J (ed) 1983 *Glassy Metals II* (Berlin: Springer)
Belitz D and Schlacher W 1984 *Proc. 5th Int. Conf. on Liquid and Amorphous Metals* (1984 *J. Non-Cryst. Solids* **61/62**)
Bieri J B, Fert A, Creuzot G and Ousset J C 1984 *Solid State Commun.* **49** 849
Blatter A and von Allman M 1985 *Phys. Rev. Lett.* **54** 2103
Chowdhury D 1986 *Spin Glasses and other Frustrated Systems* (New York: Wiley)
Cochrane R W and Strom-Olsen J O 1984 *Phys. Rev.* B **29** 1088

Cyrot-Lackmann F and Desre P(ed) 1980 Proc. 4th Int. Conf. on Liquid and Amorphous Metals (J. Physique 41 C8 1989)

REFERENCES

Cowlam N and Gardner P P 1984a *J. Phys. F: Met. Phys.* **14** 1789
___ 1984b *Proc. 5th Int. Conf. on Liquid and Amorphous Metals* (1984 *J. Non. Cryst. Solids* **61/62**)
Davies H A 1976 *Phys. Chem. Glasses* **17** 159
Egami T 1984 *Rep. Prog. Phys.* **47** 1601
Fujiwara T 1983 *J. Phys. F: Met. Phys.* **12** 661
Gallagher B L and Greig D 1982 *J. Phys. F: Met. Phys.* **12** 1721
Gallagher B L, Greig D, Howson M A and Croxon A A M 1983 *J. Phys. F: Met. Phys.* **13** 119.
Gallagher B L and Hickey B J 1985 *J. Phys. F: Met. Phys.* **15** 911
Giessen B C 1980 *Proc. 4th Int. Conf. on Liquid and Amorphous Metals* ed F Cyrot-Lackmann and P Desre (*J. Physique Coll.* **41** C8 ~~1989~~)
___ 1980 *Phys. Rev.* **21** 406
Grabow M H and Andersøn H C 1985 *J. Non-Cryst. Solids* **75** 225
Güntherodt H-J and Beck H (ed) 1981 *Glassy Metals I* (Berlin: Springer)
Hafner J 1980 *Phys. Rev.* B **21** 406
___ 1983 *Phys. Rev.* B **28** 1734
___ 1985 *J. Non-Cryst. Solids* **69** 325
Hafner J and Philipp A 1984 *J. Phys. F: Met. Phys.* **14** 1685
Hickey B J, Gallagher B L and Howson M A 1986 *J. Phys. F: Met. Phys.* **16** L13
Howson M A 1984 *J. Phys. F: Met. Phys.* **14** L25
Howson M A and Greig D 1983 *J. Phys F: Met. Phys.* **13** L155
Howson M A and Greig D 1984 *Phys. Rev.* B **30** 4805
Howson M A and Morgan G J 1985 *Phil. Mag.* B **51** 439
Hume-Rothery W, Christian J W and Pearson W B 1952 *Metallurgical Equilibrium Diagrams* (London: Chapman and Hall)
Jäckle J 1980 *J. Phys. F: Met. Phys.* **10** L43
Kaiser A B 1982 *J. Phys. F: Met. Phys.* **12** L223
Kawabata A 1982 *Solid State Commun.* **38** 823
Khanna S N, Ibrahim A K, McKnight S W and Bansil A 1985 *Solid State Commun* **55** 223
Künzi H-U and Güntherodt H-J 1980 *The Hall Effect and its Applications* (New York: Plenum)
Lapka R, Oelhafen P, Gubler U M and Güntherodt H-J 1985 *Phys. Rev.* B **31** 7734
Lasjaunias J C, Zougmore F and Béthoux O 1986 *Solid State Commun.* **60** 35
Lee P A and Ramakrishnan T V 1985 *Rev. Mod. Phys.* **57** 287
Luborsky F E (Ed) 1983 *Amorphous Metallic Alloys* (London: Butterworths)
Mizutani U 1983 *Prog. Mater. Sci.* **28** 97
Mooij J H 1973 *Phys. Status Solidi* A **17** 521
Moorjani K and Coey J M D 1984 *Magnetic Glasses* (Amsterdam: Elsevier)
Morgan G J and Howson M A 1985 *J. Phys. C: Solid State Phys.* **18** 4327
Mott N F and Davis E A 1979 *Electronic Processes in Non-Crystalline Materials* (Oxford: Clarendon)
Nagel S R and Tauc J 1975 *Phys. Rev. Lett.* **35** 380
Naugle D G, Delgado R, Armbrüster H, Tsai C L, Johnson W L and Williams A R 1985 *J. Phys. F: Met. Phys.* **15** 2189
Nguyen-Manh D, Mayou D, Morgan G J and Pasturel A 1986 in press
Nozières P and Pines D 1966 *The Theory of Quantum Liquids* (New York: Benjamin)

Olivier M, Strøm-Olsen J O, Altounian Z, Cochrane R W and Trudeau M 1986 *Phys. Rev.* B **33** 2799
Pavuna D 1981 *Phd Thesis* University of Leeds
Poon S J, Wong A M and Drehman A J 1985 *Phys. Rev.* B **31** 1668
Sakata M, Cowlam N and Davies H A 1981 *J. Phys. F: Met. Phys.* **11** L157
Sato H, Matsudo T and Mizutani U 1986 *Physica* in press
Schirmacher W 1985 *Proc. 5th Int. Conf. on Rapdily Quenched Metals* ed S Steeb and H Warlimont (Amsterdam: North-Holland) p 995
Skocpol W J and Tinkham M 1975 *Rep. Prog. Phys.* **38** 1049
Steeb S and Warlimont H (ed) 1985 *Proc. 5th Int. Conf. on Rapidly Quenched Metals* (Amsterdam: North Holland)
Strolovitz D, Egami T and Vitek V 1981 *Phys. Rev.* B **24** 6936
Suzuki K (ed) 1982 *Proc. 4th Int. Conf. on Rapidly Quenched Metals* (Sendai: Japanese Institute of Metals)
Weaire D, Ashby M F, Logan J and Weins M J 1971 *Acta Metall.* **19** 779
Wright A C, Hannon A C, Clare A G, Sinclair R N, Johnson W L, Atzman M and Mangin P 1985 *J. Physique Coll.* **46** C8 299
Wright A C, Hannon A C, Sinclair R N, Johnson W L and Atzman M 1984 *J. Phys. F: Met. Phys.* **14** L201

Wagner CNJ Johnson WL (ed) 1984 Proc. 5th Int. Conf. on Liquid and Amorphous Me (J. Non-Cryst. Solids 61/62)